the FEBS Journal

A peptide derived from the C-terminus of PB1 inhibits influenza virus replication by interfering with viral polymerase assembly

Chunfeng Li[1,2,*], Qi Ba[1,2,*], Aiping Wu[1], Hong Zhang[1], Tao Deng[3] and Taijiao Jiang[1]

1 Key Laboratory of Protein and Peptide Pharmaceutical, National Laboratory of Biomacromolecules, Institute of Biophysics, Chinese Academy of Sciences, Beijing, China
2 College of Life Sciences, University of Chinese Academy of Sciences, Beijing, China
3 MOH Key Laboratory of Systems Biology of Pathogens, Institute of Pathogen Biology, Chinese Academy of Medical Sciences & Peking Union Medical College, Beijing, China

Keywords
influenza polymerase assembly; influenza virus; peptide inhibitor; subunit interaction; virus replication

Correspondence
T. Deng or T. Jiang, MOH Key Laboratory of Systems Biology of Pathogens, Institute of Pathogen Biology, Chinese Academy of Medical Sciences & Peking Union Medical College, Beijing, 100730, China; Key Laboratory of Protein and Peptide Pharmaceutical, National Laboratory of Biomacromolecules, Institute of Biophysics, Chinese Academy of Sciences, Beijing, 100101, China
Fax: +86 10 67855618; +86 10 64888427
Tel: +86 10 67855618; +86 10 64888427
E-mail: tao.deng@ipbcams.ac.cn; taijiao@moon.ibp.ac.cn

*These authors contributed equally to this work.

(Received 16 October 2012, revised 7 December 2012, accepted 21 December 2012)

doi:10.1111/febs.12107

Efficient assembly of the influenza virus RNA-dependent RNA polymerase, a heterotrimeric complex formed by three subunits (PA, PB1 and PB2) is critical for virus replication and pathogenicity. Therefore, interfering with the assembly of the RNA-dependent RNA polymerase complex could offer novel and effective anti-influenza therapeutics. In the present study, we show that a short peptide derived from amino acids 731–757 of PB1 ($PB1_{731–757}$) can disrupt the interaction between the C-terminal part of PB1 (denoted as PB1c corresponding to $PB1_{676–757}$) and the N-terminal part of PB2 (denoted as PB2n corresponding to $PB2_{1–40}$). We further show that $PB1_{731–757}$ is capable of inhibiting viral polymerase activity and viral replication. Interestingly, we find that $PB1_{731–757}$ interacts with PB1c rather than PB2n. Furthermore, mutational analyses show that the hydrophobic sites of PB1c play an essential role in the PB1c–$PB1_{731–757}$ interaction. The characterization of the inhibitory effect of $PB1_{731–757}$ on viral polymerase activity and viral replication could offer a potential target for anti-influenza drug development.

Structured digital abstract

- PB2n physically interacts with PB1c by pull down (View interaction)
- PB2n and PB1c physically interact by bimolecular fluorescence complementation (View interaction)
- PB1 (731-757) physically interacts with PB1c by pull down (View interaction)
- PB1 (731-757) and PB1c physically interact by bimolecular fluorescence complementation (View Interaction: 1, 2, 3, 4, 5)

[Structured digital abstract was added on 11 February 2013 after original online publication]

Introduction

Influenza virus, a primary member of the Orthomyxoviridae family, is responsible for annual epidemics and occasional pandemics, including the 1918 Spanish influenza (by H1N1), the 1957 Asian influenza (H2N2), the 1968 Hong Kong influenza (H3N2) and the 2009 Swine influenza (reassorted H1N1) [1–3]

Abbreviations
BiFC, bimolecular fluorescence complementation; GFP, green fluorescent protein; GST, glutathione *S*-transferase; IL-2, interleukin-2; IL-2Rα, interleukin-2 receptor; MBP, maltose binding protein; PolI, polymerase I; RdRp, RNA-dependent RNA polymerase; YFP, yellow fluorescent protein.

outbreaks. The resurgence of this pathogen has caused enormous economic losses and numerous human deaths, making our fight against influenza virus a long-stranding challenge. Currently, the most effective methods of protecting people from influenza virus infection are vaccination and the use of antiviral drugs such as M2-ion channel inhibitors (amantadine and rimantadine) and neuraminidase inhibitors (oseltamivir and zanamivir). However, the virus has the ability to rapidly evolve either through gene mutation or gene reassortment, rendering frequent vaccine mismatches and the emergence of variants resistant to the existing anti-viral drugs [4–8]. Therefore, the development of novel therapeutics against influenza, particularly when faced with the threat of the highly pathogenic avian virus (H5N1), is urgently needed [8–10].

Given its functional essentiality for viral replication and involvement in virus pathogenicity [11–14], the RNA-dependent RNA polymerase (RdRp) complex of the influenza virus has become a potential influenza drug target [9,15–17]. The RdRp is a heterotrimeric complex composed of three subunits: PA, PB1 and PB2. The assembly of the three subunits into functional viral RdRp is one of the rate-limiting steps for influenza virus RNA synthesis and virus replication [18–20]. The polymerase subunit PB1 plays a central role in RdRp assembly [14,18,21], and thus interfaces between PB1 and PA/PB2 could be potential targets for anti-influenza drugs. In-depth analyses have found that it is the N- and C-termini of PB1 that are involved in its interactions with PA and PB2, respectively [22–24]. It has been shown previously that a peptide derived from the N-terminal 25 amino acids of PB1 (denoted as $PB1_{1–25}$) can induce the disruption of the PA–PB1 interaction and thus effectively inhibit influenza virus polymerase activity [15,25,26].

In the present study, we report the characterization of a new inhibitory short peptide of 27 amino acids derived from the very C-terminus of PB1, denoted as $PB1_{731–757}$, which can effectively inhibit influenza virus polymerase activity and virus replication. Moreover, we show that $PB1_{731–757}$ can disrupt the association of the C-terminal part of PB1 (denoted as PB1c corresponding $PB1_{676–757}$) and the N-terminal part of PB2 (denoted as PB2n corresponding to $PB2_{1–40}$). Unexpectedly, $PB1_{731–757}$ interacts with PB1c rather than PB2n. Further mutational analyses and computational modelling suggest that $PB1_{731–757}$ acts as a competitor of PB2n with respect to binding to PB1c.

Results

The short peptide $PB1_{731–757}$ is able to disrupt the interaction between PB1c and PB2n

A previous deletion study has suggested the involvement of $PB1_{731–757}$ in the assembly of PB1c and PB2n [22,24]. In the present study, we tested whether the standalone short peptide $PB1_{731–757}$ derived from H5N1 (A/goose/Guangdong/1/96) is able to disrupt the PB1c–PB2n interaction. We employed a disruption assay based on the bimolecular fluorescence complementation (BiFC) assay [27,28]. The H5N1-derived PB2n and PBlc were fused to the N-terminus (YN) and C-terminus (YC) of yellow fluorescent protein (YFP), respectively. When the YN-PB2n and YC-PB1c expression plasmids were co-transformed into yeast cells, it produced a relatively high YFP fluorescence intensity after induction, indicating a relatively strong interaction between YN-PB2n and YC-PB1c. As shown in Fig. 1A, the interaction between YN-PB2n and YC-PB1c was significantly disrupted when the self-competitor PB1c was expressed in the yeast cells, whereas there was no interference in the presence of an unrelated peptide PX or in the absence of the peptides (control). These results validated the feasibility of using the BiFC-based system to analyze the factors that affect the PB1c–PB2n association. The introduction of $PB1_{731–757}$ resulted in a reduction of ~ 15% of the fluorescence intensity ($84.26 \pm 2.75\%$, $P < 0.05$), whereas the expression levels of YN-PB2n and YC-PB1c remained constant (Fig. 1A), suggesting that $PB1_{731–757}$ can interfere with the PB1c–PB2n interaction. Furthermore, the hydrophobic residue I750 within $PB1_{731–757}$ sequence has been reported previously to be essential for the PB1c–PB2n interaction [24]. Therefore, we also examined the effect of the $PB1_{731–757}$I750N mutant on the assembly of PB1c–PB2n in the BiFC disruption assay. As expected, the presence of $PB1_{731–757}$I750N ($86.98 \pm 4.59\%$, $P > 0.05$ compared to PX) did not interfere with the interaction PB1c–PB2n as efficiently as $PB1_{731–757}$, indicating that the hydrophobic residue I750 is important for the inhibitory function of $PB1_{731–757}$ (Fig. 1A).

We further performed a competitive glutathione *S*-transferase (GST) pull-down assay to confirm the disruptive effects of $PB1_{731–757}$ and $PB1_{731–757}$I750N on the PB1c–PB2n interaction *in vitro*. Figure 1B shows that the pull-down efficiency of maltose binding protein (MBP)-tagged PB1c (MBP-PB1c) by GST-tagged PB2n (GST-PB2n) can be significantly affected by the presence of $PB1_{731–757}$ compared to the presence of the

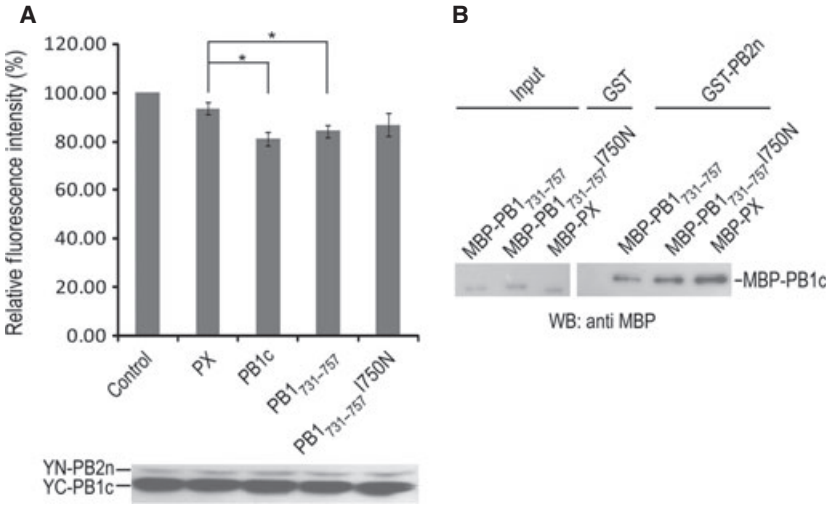

Fig. 1. The effect of $PB1_{731–757}$ on the PB1c–PB2n association. (A) The relative fluorescence intensity induced by the PB1c–PB2n interaction in the absence (control) or presence of untagged short peptides PX, PB1c, $PB1_{731–757}$ and $PB1_{731–757}$I750N was detected using the BiFC assay (upper panel). PX is an unrelated peptide from Borna disease virus phosphoprotein. $PB1_{731–757}$I750N is a derivative $PB1_{731–757}$ with the mutation I750N. All data are shown as the mean ± SD ($n = 4$). $*P < 0.05$ (Student's *t*-test) compared to PX. The expression levels of PB2n and PB1c in the presence of different short peptides were detected by western blotting with GFP polyclonal antibody (lower panel). YN-PB2n appeared to be expressed less than YC-PB1c, which may partially be a result of the lower specificity of GFP polyclonal antibody toward the YN moiety [42]. (B) GST Pull-down assay for the interaction between MBP tagged PB1c (MBP-PB1c) and GST-tagged PB2n (GST-PB2n) in the presence of $PB1_{731–757}$, $PB1_{731–757}$I750N or PX. PB1c, $PB1_{731–757}$, $PB1_{731–757}$I750N and PX were fused to the C-terminus of MBP. The input MBP-fusion proteins and eluted MBP-PB1c were analyzed by western blotting with MBP antibody. The position of MBP-PB1c is indicated.

control peptide PX, whereas $PB1_{731–757}$I750N showed less of an inhibitory effect. These results are consistent with observations made from the BiFC disruption assay. We concluded that the presence of $PB1_{731–757}$ is capable of interfering with PB1c–PB2n assembly and that the I750 of $PB1_{731–757}$ contributes to its inhibitory effect.

$PB1_{731–757}$ interacts directly with PB1c instead of PB2n

We next examined whether $PB1_{731–757}$ acts as a PB1c competitor to disrupt the interaction between PB1c and PB2n by analyzing the direct interaction between PB2n and $PB1_{731–757}$. We carried out a pull-down assay using GST-tagged $PB1_{731–757}$ (GST-$PB1_{731–757}$) to pull down MBP-tagged PB2n (MBP-PB2n), whereas the interaction between GST-PB2n and MBP-PB1c served as a positive control. To reduce the influence of fused tag to the peptide-peptide interactions, unstructured linkers between GST or MBP and our peptides were inserted. The GST pull-down assay was previously shown to be feasible with respect to detecting interactions involving peptides [29,30]. Moreover, GST or MBP can improve the solubility and stability of the fused partner [31,32]. The input amounts of these peptides in this experiment were maintained at similar levels. Unexpectedly, we found that $PB1_{731–757}$ cannot pull down PB2n, whereas the interaction between PB1c and PB2n was obvious in the pull-down assay (Fig. 2A). According to the crystal structure of the complex formed by PB1c and PB2n [24], both PB1c and $PB1_{731–757}$ show amphipathic characteristics in that they are organized as hydrophobic amino acids on the one side and hydrophilic amino acids on the other side (Fig. S1). Because PB1c contains a hydrophobic patch that can apparently accommodate an α helix, and because the hydrophobic residue I750 of $PB1_{731–757}$ is critical for the inhibitory function of $PB1_{731–757}$ (as shown above), we were interested in testing whether $PB1_{731–757}$ interacts with PB1c directly with the PB1c–PB2n interaction as a comparison. As shown in Fig. 2B (upper panel), the binding capacity of $PB1_{731–757}$ with PB1c was evident but weaker than that of PB1c and PB2n, whereas the binding capacity of $PB1_{731–757}$I750N to PB1c was very weak. Because purified GST-PB2n was unstable (Fig. 2B, lower panel), the amounts of purified GST fusion proteins were used to normalize the binding capacity between PB1c or PB2n and $PB1_{731–757}$. As shown in Fig. 2C, the relative binding strength between PB1c and $PB1_{731–757}$ was ~ 5% of that of PB1c–PB2n after normalization and there was no interaction

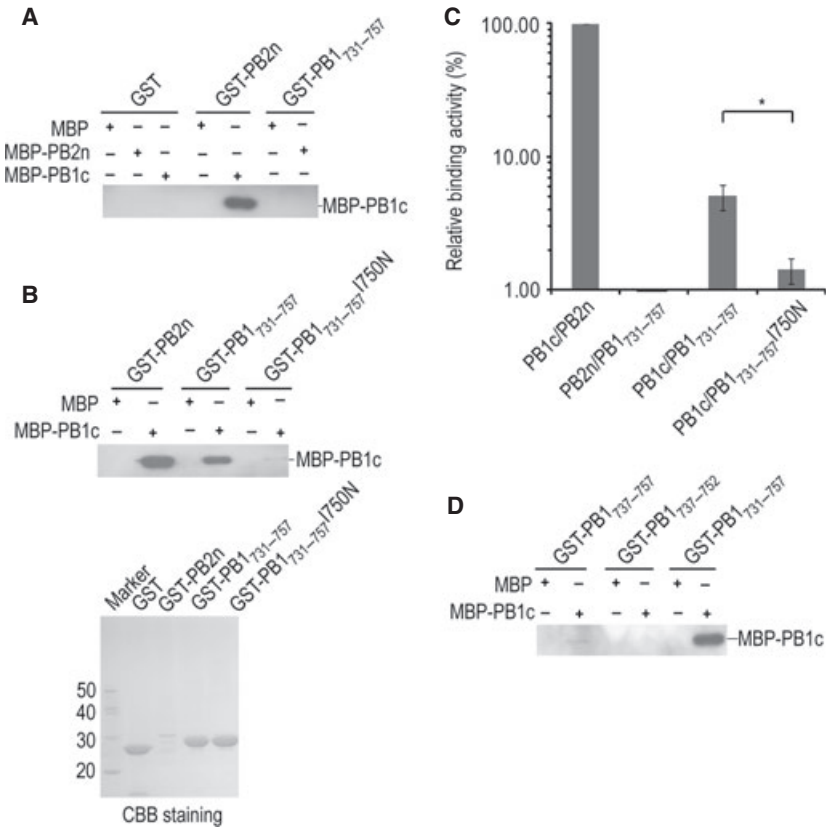

Fig. 2. Detection of the interaction between PB2n or PB1c and $PB1_{731–757}$ using the GST pull-down assay. (A) The interactions between PB2n and $PB1_{731–757}$ were detected using the GST pull-down assay. The PB1c–PB2n interaction served as a positive control. The eluted proteins were separated by SDS/PAGE and detected by western blotting with MBP antibody. The position of MBP-PB1c is indicated. (B) GST pull-down assay for the bindings between PB1c and $PB1_{731–757}$ or $PB1_{731–757}$I750N. The PB1c–PB2n interaction was conducted as a comparison (upper panel). The purified GST proteins were analyzed by Coomassie brilliant blue staining and protein markers are shown on the left (kDa) (lower panel). (C) The relative binding activities between PB2n or PB1c and $PB1_{731–757}$ or $PB1_{731–757}$I750N described in (A) and (B) were normalized by the amounts of purified GST fusion proteins noted in (B) (lower panel). The relative binding activity between PB1c and PB2n (PB1c/PB2n) was set to 100%. All data are shown as the mean ± SD ($n = 3$). (*$P < 0.05$). (D) GST pull-down assay for the interactions between PB1c and two truncations of $PB1_{731–757}$ (named $PB1_{737–757}$ and $PB1_{737–752}$).

detected between PB2n and $PB1_{731–757}$. The relative binding strength between PB1c and $PB1_{731–757}$I750N was much lower than that between PB1c and $PB1_{731–757}$ ($P < 0.05$). These results are consistent with the results obtained from both the BiFC disruption assay and the competitive GST pull-down assay.

We then conducted the BiFC assay to confirm the interaction between PB1c and $PB1_{731–757}$. The co-transformation of plasmids expressing YN-PB1c and YC-$PB1_{731–757}$ (YN-PB1c/YC-$PB1_{731–757}$) into yeast strain ySC8 gave a much higher YFP intensity than the controls (YN/YC-$PB1_{731–757}$ and YN-PB1c/YC), whereas YN-PB1c and YC-$PB1_{731–757}$I750N showed a much weaker YFP intensity, and no interaction was observed between YN-PB2n and YC-$PB1_{731–757}$ (Table 1). This is agreement with the results obtained

Table 1. BiFC results for the interactions between $PB1_{731–757}$, PB1c and PB2n. Binding activity is estimated as the ratio of relative fluorescence intensity (RRFI) of the test group compared to controls. If RRFI: ≥ 4.0, binding activity is strong (+++); < 4.0 and ≥ 2.5, binding activity is intermediate (++); < 2.5 and ≥ 1.3, binding activity is weak (+); < 1.3, there is no interaction (–).

Partner A	Partner B	Binding activity
PB2n	PB1c	+++
	$PB1_{731–757}$	–
PB1c	$PB1_{731–757}$	++
	$PB1_{731–757}$I750N	+
$PB1_{731–757}$	$PB1_{676–700}$	–
	$PB1_{701–730}$	–
	$PB1_{731–757}$	–
	$PB1c_{\Delta731–757}$	–
	$PB1c_{\Delta676–700}$	–

from the GST pull-down assay, showing that $PB1_{731–757}$ interacts with PB1c instead of PB2n.

To further define the minimal sequence of $PB1_{731–757}$ required for interaction with PB1c, we cloned two truncations of $PB1_{731–757}$ onto the C-terminus of GST, denoted as GST-$PB1_{737–757}$ and GST-$PB1_{737–752}$, and detected their PB1c binding activities using the GST pull-down assay. As shown in Fig. 2D, both deletion of the six N-terminal amino acids ($PB1_{737–757}$) and the five C-terminal amino acids ($PB1_{737–752}$) drastically disrupted that PB1c binding capacity, suggesting that $PB1_{731–757}$ is the minimal sequence required for the binding capacity of PB1c.

The full-length PB1c is critical for PB1c–$PB1_{731–757}$ binding

The crystal structure of PB1c-PB2n complex shows that PB1c contains three helices [24]. In addition to $PB1_{731–757}$, PB1c can be split into other two α helices at residue F700, named $PB1_{676–700}$ and $PB1_{701–730}$ (Figs 3 and S2). To test which helix of the three helices is responsible for the binding to $PB1_{731–757}$, we generated a series of PB1c helix deletion mutants ($PB1_{676–700}$, $PB1_{701–730}$, $PB1_{731–757}$, $PB1c_{\Delta731–757}$ and $PB1c_{\Delta676–700}$) and analyzed the interactions between these mutants and $PB1_{731–757}$ using the GST pull-down assay. As shown in Fig. 3, because the input amounts of MBP fusion proteins were on the same level, either the deletion of one helix or the deletion of the end helix of the PB1c resulted in a complete loss of $PB1_{731–757}$ binding capacity. These results were further confirmed using the BiFC assay (Table 1). Therefore, we concluded that full-length PB1c is required for its interaction with $PB1_{731–757}$, indicating that $PB1_{731–757}$ interacts with the three dimensional structure formed by all three helices of PB1c.

We further aimed to identify the key residues on PB1c that are responsible for its binding to $PB1_{731–757}$. Given the amphipathic characteristics of both PB1c and $PB1_{731–757}$ (Fig. S1), we tested the effects of several hydrophobic/hydrophilic point mutants that are spread in all three helixes of PB1c on PB1c–$PB1_{731–757}$ binding. L695, F699 and I750 of PB1c were mutated as a result of a previous study [24], showing these residues are critical for the PB1c–PB2n interaction. We also mutated another residue M718 because it is also located in the hydrophobic region of PB1c. In addition, we mutated two hydrophilic residues (R727 and K745) on the hydrophilic side of PB1c. As shown in Table 2, the mutations of the hydrophobic residues can significantly affect the interaction of PB1c with $PB1_{731–757}$: L695D and M718A substitutions completely abolished the PB1c–$PB1_{731–757}$ interaction, whereas the F699A and I750N/I750D mutations resulted in a much lower binding capacity. By contrast, the mutations of the hydrophilic amino acids R727 and K745 did not affect the binding. Taken these findings together, the hydrophobic residues of all three helixes of PB1c appear to be essential for the PB1c–$PB1_{731–757}$ interaction.

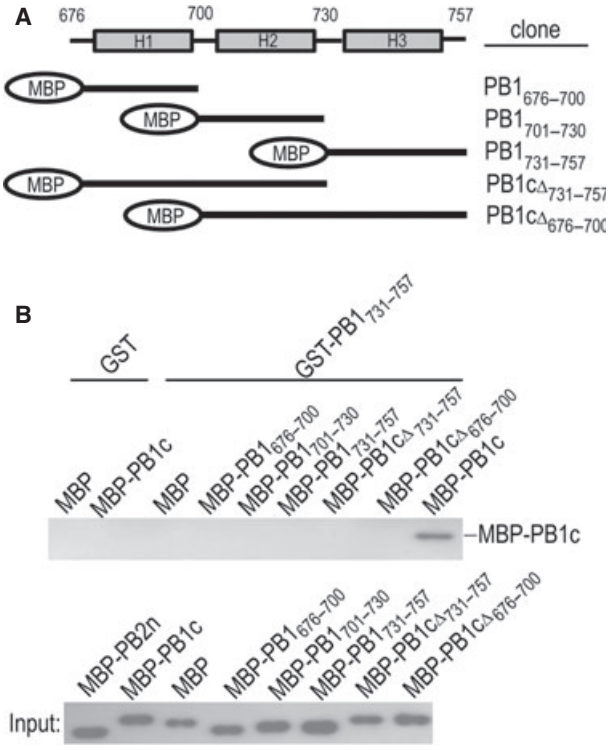

Fig. 3. Detection of the interaction between truncations of PB1c and $PB1_{731–757}$ using the GST pull-down assay. (A) Summary of constructs of PB1c truncations. Sequences of PB1c truncations are represented by black lines fused to MBP. Helices of PB1c are represented by shaded rectangles and loops are the black lines on top. Residue numbers indicate the boundary of the truncations. (B) The interaction between truncations of PB1c and $PB1_{731–757}$ was analyzed using the GST pull-down assay. The position of MBP-PB1c is labelled. The amounts of input MBP-fusion proteins are indicated by western blotting (lower panel).

The peptide $PB1_{731–757}$ is capable of inhibiting influenza RNA polymerase activity and virus replication

Based on above observations that $PB1_{731–757}$ could act as a PB2n competitor to interfere with PB1–PB2 interface assembly, we next examined whether $PB1_{731–757}$ can inhibit influenza polymerase activity and virus replication. Because the C-terminal region 686-698 of PB1 has also been reported to be involved in

Table 2. Effects of PB1c mutations on its interactions with $PB1_{731–757}$. Binding activity is estimated as the ratio of relative fluorescence intensity (RRFI) of the test group compared to controls. If RRFI: $\geq$ 4.0, binding activity is strong (+++); < 4.0 and $\geq$ 2.5, binding activity is intermediate (++); < 2.5 and $\geq$ 1.3, binding activity is weak (+); < 1.3, there is no interaction (–).

Location	Mutation	Binding activity
	WT	++
$PB1_{676–700}$	L695D	–
	F699A	+
$PB1_{701–730}$	M718A	–
	R727A	++
$PB1_{731–757}$	K745A	++
	I750N/D	+

the PB1–PB2 interaction [22], we also included a $PB1_{676–700}$ peptide that is the full sequence of the first α helix of PB1c in our analyses. In addition, $PB1_{1–25}$ was also included as a positive control [26]. We first measured their effects on polymerase activity by transfecting GFP-tagged peptide expression plasmids into 293T cells harbouring a mini-replicon system of influenza A virus (A/WSN/33). As shown in Fig. 4A (upper panel), compared to GFP-tagged Flag and GFP-tagged PX, which showed no effects on influenza replication as reported previously [15], the over-expression of GFP-tagged $PB1_{676–700}$ did not significantly affect RdRp activity, whereas GFP-tagged $PB1_{731–757}$, similar to GFP-tagged $PB1_{1–25}$, disrupted viral polymerase activity significantly. The western blotting assay of GFP expression showed that the expression levels of these peptides, except $PB1_{1–25}$, were similar (Fig. 4A, lower panel). By contrast, $PB1_{731–757}$I750N was less efficient in inhibiting polymerase activity than $PB1_{731–757}$ ($P < 0.01$), Therefore, we concluded that $PB1_{731–757}$ is able to inhibit viral RNA polymerase activity, which is consistent with its inhibitory effect on the assembly of PB1c–PB2n.

To further analyze whether the peptide $PB1_{731–757}$ can inhibit influenza virus replication in cells, we used a reporter system based on secreted *Gaussia* luciferase [33] to monitor influenza virus infection in the presence of $PB1_{731–757}$-GFP. We also included the peptide $PB1_{1–25}$ reported by Ghanem *et al*. as a comparison [26]. As shown in Fig. 4B, $PB1_{731–757}$, similar to $PB1_{1–25}$, can effectively block the replication of human influenza virus A/WSN/33 (H1N1).

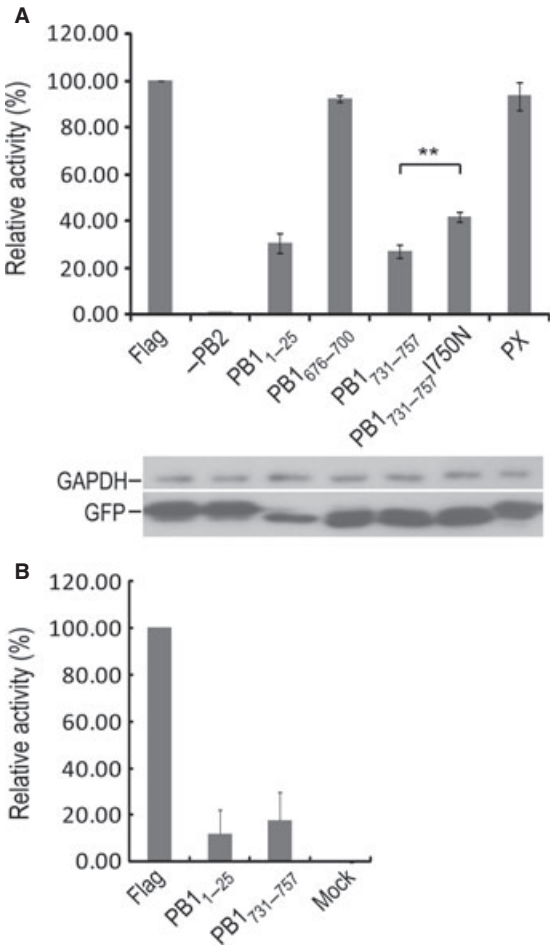

Fig. 4. The over-expression of $PB1_{731–757}$ inhibits influenza virus polymerase activity and virus replication. (A) Effects of over-expressed short peptides on influenza A virus polymerase activity (upper panel). The viral polymerase activity was assayed in a mini-replicon system of A/WSN/33 (H1N1) with a Poll-driven plasmid expressing influenza virus-like RNA coding for firefly luciferase to detect viral polymerase activity. The short peptides were expressed as GFP fusions. Plasmid expressing *Renilla* luciferasse was also included in transfection used to normalize transfection efficiency. '-PB2' indicates the omission of PB2 from the transfection mixture, which served as a negative control. $PB1_{1–25}$-GFP ($PB1_{1–25}$), which has been reported to inhibit polymerase activity, served as a positive control. The polymerase activities are expressed as activity relative to that under Flag expression (Flag), which is set as 100%. All data are shown as the mean ± SD. $^{**}P < 0.01$ (Student's *t*-test) ($n = 3$). The expression levels of GFP fusion proteins and glyceraldehyde 3-phosphate dehydrogenase were detected by western blotting with the indicated antibodies (lower panel). (B) Effect of over-expressed $PB1_{731–757}$ on virus replication activity of A/WSN/33. The assay is performed in A549 cells using the *Gaussia* luciferase reporter system. $PB1_{1–25}$-GFP ($PB1_{1–25}$) and Flag-GFP (Flag) were used as positive and negative controls, respectively. The luciferase activity under the expression of Flag-GFP (Flag) is set as 100% after subtracting the background of uninfected cells ('Mock'). All data are shown as the mean ± SD ($n = 3$).

Discussion

The influenza virus RdRp is responsible for viral RNA transcription and replication in the nucleus of infected cells. The efficiency of viral RNA synthesis, which is critical for virus replication and pathogenicity, is depen-

dent on the RNP assembly and RdRp activity. Given that its functionality requires the proper assembly of the three subunits, the modulation of RdRp assembly can effectively affect its activity, and thus could prove to be a very promising avenue for the development of effective therapeutics against this highly elusive pathogen.

Previously, short peptides derived from polymerase subunits were shown to inhibit virus replication by interfering with polymerase assembly. For example, the $PB1_{1–25}$ peptide can disrupt any interaction between PA and PB1 efficiently, and $PB2_{1–12}$ can inhibit influenza virus polymerase activity in a strain-specific manner [15,17,26]. In the present study, we characterized another novel potent inhibitory peptide, $PB1_{731–757}$, derived from the C-terminus of PB1, which can disrupt the assembly of PB1c and PB2n and inhibit influenza RdRp activity, and thus virus replication, as efficiently as $PB1_{1–25}$.

Interestingly, the data obtained in the present study show that the inhibitory effect of $PB1_{731–757}$ on the PB1c–PB2n interaction acts through its binding to the PBlc, from where it derives, rather than PB2n. Moreover, we find that the inhibitory binding is mainly mediated by the hydrophobic interactions between the PB1c and $PB1_{731–757}$. This is different from the inhibitory mechanism of the interfacial peptides $PB1_{1–25}$ and $PB2_{1–12}$, which inhibit complex assembly by binding to its interaction partner PAc or PB1c, respectively [15,17,23–26,34]. Similar to the findings of the present study, an inhibitory mechanism has been reported for Ro26-4550 with respect to interfering with the interaction between interleukin-2 (IL-2) and its receptor (IL-2Rα). The Ro26-4550 was designed as a peptidomimetic of the IL-2Rα binding site on IL-2 to interfere with the assembly of IL-2 and IL-2Rα, although it actually interacts with IL-2 rather than IL-2Rα by hydrophobic interactions [35,36].

Based on the crystal structure of the PB1c and our observation that the hydrophobic region of PB1c is critical for the PB1c–$PB1_{731–757}$ interaction, we modelled the complex structure of PB1c–$PB1_{731–757}$ using a site-constrained docking method [37]. There is no structure for H5N1 PB1c and there are only three different residues between A/Puerto Rico/8/34 (H1N1) PB1c and A/goose/Guangdong/1/96 (H5N1) PB1c, as shown in Fig. S3A, which are away from the hydrophobic patch of PB1c. Thus, that structure of A/Puerto Rico/8/34 PB1c was used in our docking assay. As shown in Fig. 5A, $PB1_{731–757}$ can be buried in the hydrophobic grove formed by the hydrophobic residues located in three helices of PB1c. Furthermore, the side chains of hydrophobic residues on $PB1_{731–757}$ are all towards to the hydrophobic patch of PB1c, as shown in Fig. S4. Therefore, we speculate that the previously reported PB2n-derived peptide $PB2_{1–12}$ may also interact with PB1c in a similar way as $PB1_{731–757}$ does because it has been also shown that hydrophobic interactions between PB1c and $PB2_{1–12}$ are critical for their interaction [17,24]. The PB1c–PB2n complex was aligned to the PB1c–$PB1_{731–757}$ complex with PYMOL (http://www.pymol.org/) based on the PB1c structures. Both PB1c structures aligned well and only the structure of PB1c from the PB1c–$PB1_{731–757}$ complex was shown. Figure 5B shows that $PB1_{731–757}$ overlapped with the first α helix of PB2n ($PB2_{1–12}$), whereas the directions of the two helixes are different. This is consistent with the fact that $PB2_{1–12}$ contributes most of the binding energy between PB1c and PB2n [24]. It can also be seen that the first α helix of PB2n is much closer to the hydrophobic patch of PB1c than $PB1_{731–757}$, which correlates with the results indicating that the relative binding activity between PB1c and PB2n is much higher than that between PB1c and $PB1_{731–757}$ (Fig. 2C and Table 1). However, we found

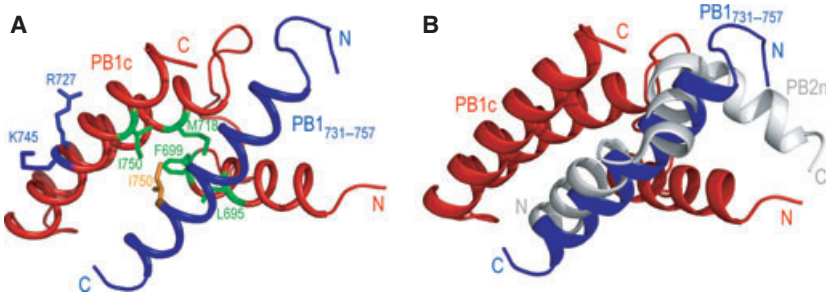

Fig. 5. Structural model of PB1c–$PB1_{731–757}$ complex and its structural alignment with the PB1c–PB2n complex. (A) An overall ribbon diagram showing the docking model of the complex: PB1c coloured red and $PB1_{731–757}$ coloured light blue. Experimental mutants are marked on the docking model. I750 from $PB1_{731–757}$ is coloured yellow; the hydrophobic residues L695, F699, M718 and I750 on PB1c are coloured green; and the hydrophilic residues R727 and K745 are coloured dark blue. The N- and C-termini are indicated. (B) The structural alignment between the PB1c–PB2n complex and the PB1c–$PB1_{731–757}$ complex with PYMOL based on the PB1c structures. PB1c from PB1c–$PB1_{731–757}$, $PB1_{731–757}$ and PB2n are coloured red, blue and grey, respectively. The N- and C-termini are indicated.

that the PB1c-derived $PB1_{676–700}$ could not inhibit viral RNA polymerase activity (Fig. 4A). To explore the possible reasons for this, we analyzed the hydrophobic surface of $PB1_{684–700}$ because the structure of PB1c started from residue E684 based on the reported three-dimensional structure of PB1c and PB2n (Fig. S5). The structure shows that the hydrophobic surface of $PB1_{684–700}$ is different from that of $PB1_{731–757}$. The C-terminus of $PB1_{684–700}$ lacks hydrophilic amino acids, whereas $PB1_{731–757}$ has hydrophilic amino acids on both termini. As shown in Figs 2D and S1B, both hydrophilic termini of $PB1_{731–757}$ contribute to the PB1c–$PB1_{731–757}$ interaction. In addition, the hydrophobic area of $PB1_{684–700}$ is smaller than that of $PB1_{731–757}$. These findings might explain why $PB1_{676–700}$ cannot form a similar tertiary structure with PB1c and thus inhibit polymerase activity. Furthermore, amino acid sequence alignment of the three peptides ($PB1_{676–700}$, $PB1_{731–757}$ and $PB2_{1–27}$) shows that $PB1_{731–757}$ and $PB2_{1–27}$ share a larger number of conserved amino acids, whereas $PB1_{676–700}$ does not (Fig. S3B). We consider that additional screening of the small molecules that specifically target the hydrophobic grove of the PB1c may identify potent drugs that act against the influenza virus.

Materials and methods

Cells and plasmids

HEK293T and A549 cells were maintained as described previously [33]. pPolI-NP-luc, pPolI-Gluc and cDNA of influenza A/goose/Guangdong/1/96 (H5N1) were generously provided by Professor Martin Schwemmle (University of Freiburg, Germany), Professor Yuelong Shu (Center for Disease Control and Prevention, Beijing, China) and Professor Yingfang Liu (Chinese Academy of Sciences, Beijing, China), respectively.

BiFC assay

The BiFC assay was conducted as described previously [38,39]. Briefly, two proteins/peptides of interest were fused to the N-part (amino acids 1–154; YN) and C-part (amino acids 155–238; YC) of YFP, respectively. The plasmids expressing both fusion proteins were transformed into the cells of yeast strain ySC8. After induction in SCGR/-Leu/-Trp medium at 20 °C for 24 h, the fluorescence intensities (excitation = 485 nm, emission = 535 nm) and cell density (D_{595}) were detected using a microplate reader (GENios Plus, Tecan Group Ltd, Männedorf, Switzerland). The assays were conducted with three repeats, and the ratio of relative fluorescence intensity of test group to controls was estimated as the relative binding strength.

BiFC disruption assay

The peptides PB1c (corresponding to $PB1_{676–757}$), $PB1_{731–757}$, $PB1_{731–757}$I750N derived from PB1 of avian H5N1 A/goose/Guangdong/1/96 and an unrelated peptide PX derived from Borna disease virus phosphoprotein [15] were cloned into pYes260 [40] between the *Nar*I and *Xba*I sites under the *Gal*I promoter without introducing fusion tags onto these peptides. Next, they were transformed individually into yeast cells with plasmids expressing the interacting pair YN-PB2n (corresponding to YN-$PB2_{1–40}$) and YC-PB1c. After culturing in SCGR/-Leu/-Trp/-Ura medium at 20 °C for 24 h, the fluorescence intensities and cell density of the yeast were detected as described above. The relative fluorescence intensities of yeast cells in the absence of peptide were set to 100% (control). The SD was obtained from four independent tests with three repeats of every sample in every single independent test. The expressions of YN-PB2n and YC-PB1c were analyzed by western blotting with GFP polyclonal antibody.

GST pull-down assay

PCR products of peptides were cloned into pGEX6p-1 (GE Healthcare, Milwaukee, WI, USA) or pMal-C2-TEV (New England Biolabs, Beverly, MA, USA) to express GST- or MBP-fusion proteins, respectively, in *Escherichia coli* BL21 (DE3). GST fusion proteins were purified first and then mixed with cell lysates containing the same amounts of MBP fusion proteins at 4 °C overnight. Then the sepharoses were washed twice with NaCl/P_i and eluted with 10 mM reduced glutathione in 50 mM Tris-HCl (pH 8.0). Eluted proteins were subjected to SDS/PAGE followed by Coomassie brilliant blue staining or western blotting with anti-MBP sera. A competitive GST pull-down assay was conducted by incubating purified GST-PB2n with cell lysates containing MBP-PB1c and competitor MBP fusion peptides at 4 °C overnight. Eluted MBP-PB1c was analyzed by western blotting.

Site-directed mutagenesis

Site mutations on PB1c were generated by site-directed mutagenesis using PfuUltra (Stratagene, La Jolla, CA, USA). Plasmid expressing YN-PB1c was used as a template. Positive clones were verified by sequencing.

Reconstitution of influenza A virus polymerase activity

293T cells were transfected using poly(ethylenimine) reagent (Sigma, St Louis, MO, USA) in six-well plates. The transfection mixture contained plasmids expressing A/WSN/33-derived PB2, PB1, PA, NP and a luciferase reporter plasmid, which are all needed for the mini-replicon system

of influenza A virus [26,41]. The plasmids expressing GFP-tagged peptides and plasmids expressing *Renilla* luciferase were also added to each well. The reporter plasmid pPolI-NP-luc is a polymerase I (PolI)-driven plasmid expressing influenza virus-like firefly luciferase RNA with a noncoding region of nucleoprotein gene of influenza A virus on both ends, which was used to detect the activity of influenza A virus RdRp as described previously [26,41]. *Renilla* luciferase was used as an indication of transfection efficiency. Twenty-four hours after transfection, the firefly luciferase and *Renilla* luciferase activities of cell lysates were measured using the Dual-Glu Luciferase Assay system (Promega, Madison, WI, USA). The firefly luciferase activity of samples containing Flag-GFP after normalization by *Renilla* luciferase was set to 100%. The expression of GFP-tagged proteins and glyceraldehyde 3-phosphate dehydrogenase was detected by western blotting.

Virus infection

Influenza virus A/WSN/33 was prepared as described previously [33]. A549 cells in 24 well-plates were transfected with 1 μg of plasmids encoding GFP-tagged peptides and 0.4 μg of plasmid pPolI-Gluc, which is a PolI-driven plasmid expressing influenza virus-like RNA coding for *Gaussia* luciferase as a reporter for viral polymerase activity [33]. Twelve hours after transfection, cells were infected with A/WSN/33 virus (multiplicity of infection = 0.015) for 1.5 h. Next, cells were washed in NaCl/P_i and incubated in DMEM with 1 $\mu g \cdot mL^{-1}$ trypsin at 37 °C. Twelve hours after infection, the supernatant were collected and tested using a Gluc Assay Kit (New England Biolabs). After subtracting the background of uninfected cells ('Mock'), the luciferase activity of samples containing Flag-GFP was set to 100%.

PB1c–$PB1_{731–757}$ complex modelling

First, the structures of PB1c and $PB1_{731–757}$ were built by taking coordinates from the complex structure of PB1c–PB2n (Protein Data Bank code: 2ZTT). Then, the three sites (I750 of $PB1_{731–757}$, L695 and I750 of PB1c) were used as interface constraints to direct the docking between PB1c and $PB1_{731–757}$ using PATCHDOCK [37]. The final complex model was selected according to the docking scores and an additional rule proposing that the deletion of the six N-terminal amino acids of $PB1_{731–757}$ will weaken the interaction between PB1c and $PB1_{731–757}$. Structural alignment between the PB1c–PB2n complex and PB1c–$PB1_{731–757}$ complex was analyzed using PYMOL (version 1.5.0.4) based on the PB1c structures.

Acknowledgements

This work was supported by the National Foundation of Talent Youth (No. 31125016) and the Project '973' (No. 2009CB918503), National Key Laboratory Open Foundation (No. 2010KF04) to T.J., as well as the Chinese Science and Technology Major Project (No. 2008ZX10004-016, 2013ZX10004061-002), National Natural Science Foundation of China (No. 31070152), the project '973' (No. 2010CB534003) and an Intramural Grant from the Institute of Pathogen Biology, Chinese Academy of Medical Sciences to T.D. (No. 2009IPB201). The funders had no role in the study design, data collection and analyses, the decision to publish or the preparation of the manuscript. We thank Dr Martin Schwemmle, Yuelong Shu and Yingfang Liu for providing plasmids and also members of our Laboratory for useful discussions.

References

1 Tumpey TM & Belser JA (2009) Resurrected pandemic influenza viruses. *Annu Rev Microbiol* **63**, 79–98.
2 Stamboulian D, Bonvehi PE, Nacinovich FM & Cox N (2000) Influenza. *Infect Dis Clin North Am* **14**, 141–166.
3 Hampson AW & Mackenzie JS (2006) The influenza viruses. *Med J Aust* **185**, S39–S43.
4 Du X, Dong L, Lan Y, Peng Y, Wu A, Zhang Y, Huang W, Wang D, Wang M, Guo Y *et al.* (2012) Mapping of H3N2 influenza antigenic evolution in China reveals a strategy for vaccine strain recommendation. *Nat Commun* **3**, 709.
5 de Jong JC, Beyer WE, Palache AM, Rimmelzwaan GF & Osterhaus AD (2000) Mismatch between the 1997/1998 influenza vaccine and the major epidemic A (H3N2) virus strain as the cause of an inadequate vaccine-induced antibody response to this strain in the elderly. *J Med Virol* **61**, 94–99.
6 Nelson MI & Holmes EC (2007) The evolution of epidemic influenza. *Nat Rev Genet* **8**, 196–205.
7 Arino J, Bowman CS & Moghadas SM (2009) Antiviral resistance during pandemic influenza: implications for stockpiling and drug use. *BMC Infect Dis* **9**, 8.
8 Colman PM (2009) New antivirals and drug resistance. *Annu Rev Biochem* **78**, 95–118.
9 Boltz DA, Aldridge JR Jr, Webster RG & Govorkova EA (2010) Drugs in development for influenza. *Drugs* **70**, 1349–1362.
10 Salomon R & Webster RG (2009) The influenza virus enigma. *Cell* **136**, 402–410.
11 Hulse-Post DJ, Franks J, Boyd K, Salomon R, Hoffmann E, Yen HL, Webby RJ, Walker D, Nguyen TD & Webster RG (2007) Molecular changes in the polymerase genes (PA and PB1) associated with high pathogenicity of H5N1 influenza virus in mallard ducks. *J Virol* **81**, 8515–8524.

12 Zhou B, Li Y, Halpin R, Hine E, Spiro DJ & Wentworth DE (2011) PB2 residue 158 is a pathogenic determinant of pandemic H1N1 and H5 influenza a viruses in mice. *J Virol* **85**, 357–365.
13 Salomon R, Franks J, Govorkova EA, Ilyushina NA, Yen HL, Hulse-Post DJ, Humberd J, Trichet M, Rehg JE, Webby RJ *et al.* (2006) The polymerase complex genes contribute to the high virulence of the human H5N1 influenza virus isolate A/Vietnam/1203/04. *J Exp Med* **203**, 689–697.
14 Ruigrok RW, Crepin T, Hart DJ & Cusack S (2010) Towards an atomic resolution understanding of the influenza virus replication machinery. *Curr Opin Struct Biol* **20**, 104–113.
15 Wunderlich K, Mayer D, Ranadheera C, Holler AS, Manz B, Martin A, Chase G, Tegge W, Frank R, Kessler U *et al.* (2009) Identification of a PA-binding peptide with inhibitory activity against influenza A and B virus replication. *PLoS One* **4**, e7517.
16 Su CY, Cheng TJ, Lin MI, Wang SY, Huang WI, Lin-Chu SY, Chen YH, Wu CY, Lai MM, Cheng WC *et al.* (2010) High-throughput identification of compounds targeting influenza RNA-dependent RNA polymerase activity. *Proc Natl Acad Sci USA* **107**, 19151–19156.
17 Reuther P, Manz B, Brunotte L, Schwemmle M & Wunderlich K (2011) Targeting of the influenza A virus polymerase PB1-PB2 interface indicates strain-specific assembly differences. *J Virol* **85**, 13298–13309.
18 Deng T, Sharps J, Fodor E & Brownlee GG (2005) In vitro assembly of PB2 with a PB1-PA dimer supports a new model of assembly of influenza A virus polymerase subunits into a functional trimeric complex. *J Virol* **79**, 8669–8674.
19 Huet S, Avilov SV, Ferbitz L, Daigle N, Cusack S & Ellenberg J (2010) Nuclear import and assembly of influenza A virus RNA polymerase studied in live cells by fluorescence cross-correlation spectroscopy. *J Virol* **84**, 1254–1264.
20 Manz B, Gotz V, Wunderlich K, Eisel J, Kirchmair J, Stech J, Stech O, Chase G, Frank R & Schwemmle M (2011) Disruption of the viral polymerase complex assembly as a novel approach to attenuate influenza A virus. *J Biol Chem* **286**, 8414–8424.
21 Ohtsu Y, Honda Y, Sakata Y, Kato H & Toyoda T (2002) Fine mapping of the subunit binding sites of influenza virus RNA polymerase. *Microbiol Immunol* **46**, 167–175.
22 Poole EL, Medcalf L, Elton D & Digard P (2007) Evidence that the C-terminal PB2-binding region of the influenza A virus PB1 protein is a discrete alpha-helical domain. *FEBS Lett* **581**, 5300–5306.
23 He X, Zhou J, Bartlam M, Zhang R, Ma J, Lou Z, Li X, Li J, Joachimiak A, Zeng Z *et al.* (2008) Crystal structure of the polymerase PA(C)-PB1(N) complex from an avian influenza H5N1 virus. *Nature* **454**, 1123–1126.
24 Sugiyama K, Obayashi E, Kawaguchi A, Suzuki Y, Tame JR, Nagata K & Park SY (2009) Structural insight into the essential PB1-PB2 subunit contact of the influenza virus RNA polymerase. *EMBO J* **28**, 1803–1811.
25 Chase G, Wunderlich K, Reuther P & Schwemmle M (2011) Identification of influenza virus inhibitors which disrupt of viral polymerase protein-protein interactions. *Methods* **55**, 188–191.
26 Ghanem A, Mayer D, Chase G, Tegge W, Frank R, Kochs G, Garcia-Sastre A & Schwemmle M (2007) Peptide-mediated interference with influenza A virus polymerase. *J Virol* **81**, 7801–7804.
27 Morell M, Czihal P, Hoffmann R, Otvos L, Aviles FX & Ventura S (2008) Monitoring the interference of protein-protein interactions in vivo by bimolecular fluorescence complementation: the DnaK case. *Proteomics* **8**, 3433–3442.
28 Hu CD, Chinenov Y & Kerppola TK (2002) Visualization of interactions among bZIP and Rel family proteins in living cells using bimolecular fluorescence complementation. *Mol Cell* **9**, 789–798.
29 Wang JG, Chen CH, Chien CT & Hsieh HL (2011) FAR-RED INSENSITIVE219 modulates CONSTITUTIVE PHOTOMORPHOGENIC1 activity via physical interaction to regulate hypocotyl elongation in Arabidopsis. *Plant Physiol* **156**, 631–646.
30 Deng Q, Zhai JW, Michel ML, Zhang J, Qin J, Kong YY, Zhang XX, Budkowska A, Tiollais P, Wang Y *et al.* (2007) Identification and characterization of peptides that interact with hepatitis B virus via the putative receptor binding site. *J Virol* **81**, 4244–4254.
31 Hammarstrom M, Hellgren N, van Den Berg S, Berglund H & Hard T (2002) Rapid screening for improved solubility of small human proteins produced as fusion proteins in Escherichia coli. *Protein Sci* **11**, 313–321.
32 Waugh DS (2005) Making the most of affinity tags. *Trends Biotechnol* **23**, 316–320.
33 Zhu W, Zhou J, Qin K, Du N, Liu L, Yu Z, Zhu Y, Tian W, Wu X & Shu Y (2011) A reporter system for assaying influenza virus RNP functionality based on secreted Gaussia luciferase activity. *Virol J* **8**, 29.
34 Obayashi E, Yoshida H, Kawai F, Shibayama N, Kawaguchi A, Nagata K, Tame JR & Park SY (2008) The structural basis for an essential subunit interaction in influenza virus RNA polymerase. *Nature* **454**, 1127–1131.
35 Emerson SD, Palermo R, Liu CM, Tilley JW, Chen L, Danho W, Madison VS, Greeley DN, Ju G & Fry DC (2003) NMR characterization of interleukin-2 in complexes with the IL-2Ralpha receptor component,

and with low molecular weight compounds that inhibit the IL-2/IL-Ralpha interaction. *Protein Sci* **12**, 811–822.
36 Wilson CG & Arkin MR (2011) Small-molecule inhibitors of IL-2/IL-2R: lessons learned and applied. *Curr Top Microbiol Immunol* **348**, 25–59.
37 Schneidman-Duhovny D, Inbar Y, Nussinov R & Wolfson HJ (2005) PatchDock and SymmDock: servers for rigid and symmetric docking. *Nucleic Acids Res* **33**, W363–W367.
38 Zhang H, Chen J, Wang Y, Peng L, Dong X, Lu Y, Keating AE & Jiang T (2009) A computationally guided protein-interaction screen uncovers coiled-coil interactions involved in vesicular trafficking. *J Mol Biol* **392**, 228–241.
39 Wang Y, Zhang X, Zhang H, Lu Y, Huang H, Dong X, Chen J, Dong J, Yang X, Hang H *et al.* (2012) Coiled-coil networking shapes cell molecular machinery. *Mol Biol Cell* **23**, 3911–3922.
40 Melcher K (2000) A modular set of prokaryotic and eukaryotic expression vectors. *Anal Biochem* **277**, 109–120.
41 Fodor E, Devenish L, Engelhardt OG, Palese P, Brownlee GG & Garcia-Sastre A (1999) Rescue of influenza A virus from recombinant DNA. *J Virol* **73**, 9679–9682.
42 Ohad N, Shichrur K & Yalovsky S (2007) The analysis of protein-protein interactions in plants by bimolecular fluorescence complementation. *Plant Physiol* **145**, 1090–1099.

Supporting information

Additional supporting information may be found in the online version of this article at the publisher's web site:

Fig. S1. Surface view of the hydrophobic region on PB1c (A) and $PB1_{731–757}$ (B).

Fig. S2. The location of three helices on PB1c.

Fig. S3. Amino acid sequence alignment between PB1c from A/Puerto Rico/8/34 (H1N1) and A/goose/Guangdong/1/96 (H5N1) (A), $PB1_{676–700}$, $PB1_{731–757}$ and $PB2_{1–27}$ from A/goose/Guangdong/1/96 (B).

Fig. S4. The location of the hydrophobic residues on $PB1_{731–757}$ of PB1c–$PB1_{731–757}$ complex.

Fig. S5. The hydrophobic surface analyses of $PB1_{684–700}$.